



## Multidecadal and multicentennial variability of the meridional overturning circulation

W. Park<sup>1</sup> and M. Latif<sup>1</sup>

Received 22 August 2008; revised 2 October 2008; accepted 10 October 2008; published 20 November 2008.

[1] The variability of the meridional overturning circulation (MOC) simulated in a multimillennial control integration of the Kiel Climate Model (KCM) displays enhanced variability relative to the red background at decadal and centennial timescales. The multidecadal variability is the model's version of the Atlantic Multidecadal Variability (AMV), often referred to as Atlantic Multidecadal Oscillation (AMO). While multidecadal variability originates in the North Atlantic, multicentennial variability is driven in the Southern Ocean. Both multidecadal and multicentennial variability are associated with considerable changes in sea ice extent. This may be important to understand the different evolution of sea ice cover in the Northern and Southern Hemisphere during the most recent decades, with a strong decline observed in the North and almost no trend in the South. **Citation:** Park, W., and M. Latif (2008), Multidecadal and multicentennial variability of the meridional overturning circulation, *Geophys. Res. Lett.*, 35, L22703, doi:10.1029/2008GL035779.

### 1. Introduction

[2] The Atlantic Ocean is unique as it displays a basin wide meridional overturning circulation (MOC) (see, e.g., Schmittner *et al.* [2007] for a review). Long control integrations of climate models have been used to obtain insight into the dynamics of MOC variability [e.g., Delworth *et al.*, 1993; Timmermann *et al.*, 1998; Delworth and Mann, 2000; Latif *et al.*, 2004; Knight *et al.*, 2005, 2006]. Such models simulate MOC variability on a wide range of timescales, from monthly to centennial. However, only a rudimentary picture exists about the dynamics of MOC variability from observations. In recent years, large efforts were made to improve the situation and results were reported by, for example, Kanzow *et al.* [2007] about the mean MOC at 26.5°N and by Cunningham *et al.* [2007] about its variability using a variety of measurements including the RAPID Climate Change array. In spite of this progress, the observational database remains poor, especially when addressing the characteristics of long-term MOC variability on decadal and longer timescales. Latif *et al.* [2004] showed a rather strong connection between indices of MOC and North Atlantic SST in a multicentury control integration of a climate model. This was followed up by Latif *et al.* [2006], who reconstructed the relative MOC changes during the 20th century with observed Atlantic sea surface temperature (SST). They used the inter-hemispheric SST dipole, a pattern with opposite polarities in the North and South

Atlantic [e.g., Folland *et al.*, 1986], as a fingerprint of MOC change and report strong multidecadal variability with an increase in MOC strength from the 1970s to the 1990s. This, although supported by forced ocean model simulations [Latif *et al.*, 2007], can be considered only as a very crude estimate of the multidecadal MOC variability. The bipolarity plays also an important role in paleo-climatic studies to explain the asynchrony of Antarctic and Greenland climate change during the last glacial period [e.g., Stocker, 1998; EPICA Community Members, 2006].

[3] The strong multidecadal or even longer-timescale variability may mask anthropogenic climate signals which evolve on similar timescales. Latif *et al.* [2006], for instance, concluded that expected anthropogenic weakening of the MOC may not be detectable during the next decades due to the presence of strong internal multidecadal variability. This may not only apply to the MOC itself but also to other potentially related quantities such as Sahel rainfall or Atlantic hurricane activity. Both are also characterized by pronounced multidecadal variability [e.g., Zhang and Delworth, 2006], which may hinder early detection of an anthropogenic signal. One observation deserves attention in this context: while Northern Hemisphere sea ice extent exhibits a fast decline since the late 1970s, Southern Hemisphere sea ice extent does not show any sustained long-term trend and even slightly increased in recent years. We expect a considerable retreat of sea ice extent in both hemispheres by the end of the 21st century in response to global warming, but low-frequency MOC variability and related sea ice changes may have masked this up to present. Here we investigate the results from a multimillennial control integration of the Kiel Climate Model in order to explore the level of internally generated MOC variability up to centennial timescales, to identify the differences between multidecadal and multicentennial variability, and to discuss the implications for global change detection, specifically with respect to Northern and Southern Hemisphere sea ice extent.

### 2. Model and Data

[4] The Kiel Climate Model (KCM) described in detail by Park *et al.* [2008] consists of the ECHAM5 [Roeckner *et al.*, 2003] atmosphere general circulation model coupled to the NEMO [Madec *et al.*, 1998; Madec, 2008] ocean-sea ice general circulation model, with the OASIS3 coupler [Valcke, 2006]. No form of flux correction or anomaly coupling is used. The atmospheric resolution is T31 (3.75° × 3.75°) horizontally with 19 vertical levels. The horizontal ocean resolution is based on a 2° Mercator mesh and is on average 1.3°, with enhanced meridional resolution of 0.5° in the equatorial region. KCM was integrated for 5000 years in total using the same model version described by Park *et al.*

<sup>1</sup>Leibniz-Institut für Meereswissenschaften, Kiel, Germany.

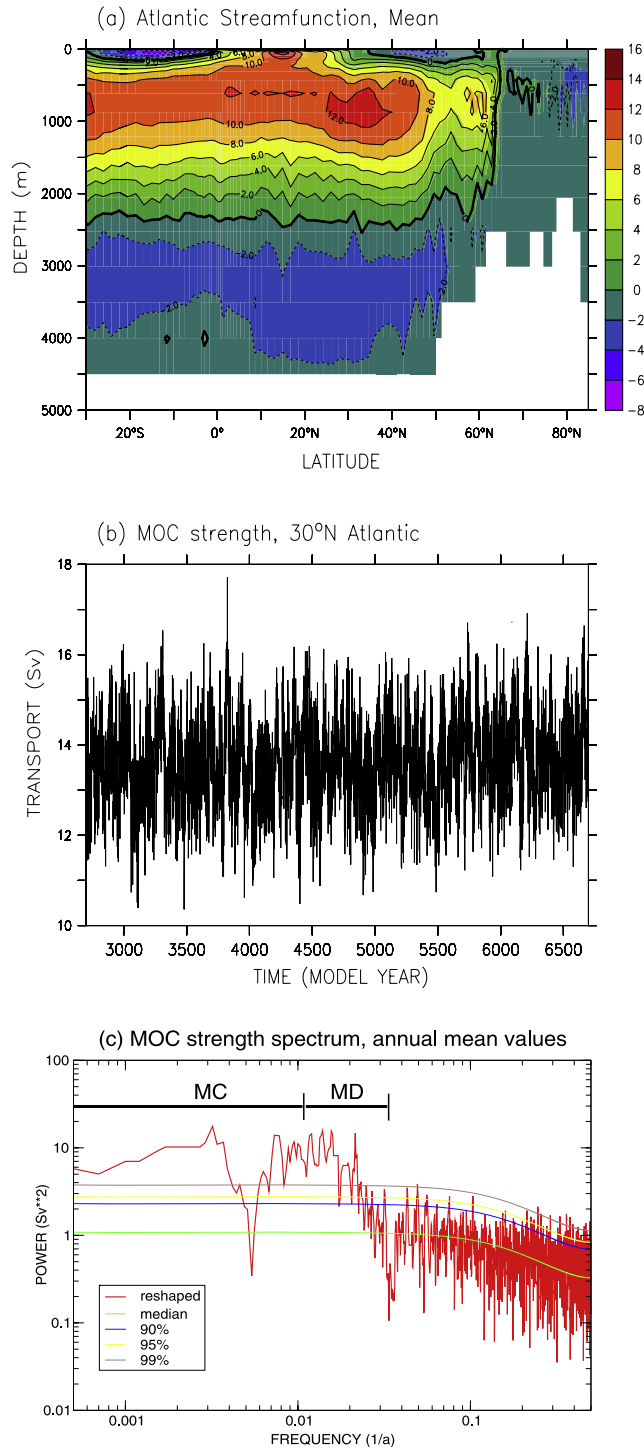


**Figure 1.** (a) Mean MOC [Sv] averaged over all 4000 years, (b) timeseries of MOC strength [Sv] defined as the maximum of the stream function at  $30^{\circ}\text{N}$  based on annual averages ( $\sigma = 1.02\text{Sv}$ ), and (c) power spectrum of the MOC strength [ $\text{Sv}^2$ ] as function of frequency [ $1/\text{a}$ ]. The multicentennial (MC) and multidecadal bands (MD) are denoted by horizontal lines.

[2008] but with slightly different parameters. We consider here only the last 4000 years after skipping the initial 1000 years to account for model spin up. Annual data from

the integration are used which were averaged to 5-year means for specific analyses.

[5] Model biases were discussed by *Park et al.* [2008]. Of particular importance here is the simulation of the MOC and sea ice. The maximum of the overturning stream function (Figure 1a) at  $30^{\circ}\text{N}$  amounts to about  $14\text{Sv}$  ( $1\text{Sv} = 10^6 \text{ m}^3/\text{s}$ ). Observational estimates at  $25^{\circ}\text{N}$ , however, reveal somewhat larger values of about  $15.75 \pm 1.6\text{Sv}$  [*Schmittner et al.*, 2005]. We next compare the extremes of the annual cycle of sea ice extent. Minimum Arctic sea ice extent amounts to about  $6 \cdot 10^6 \text{ km}^2$  and maximum ice extent to about  $17 \cdot 10^6 \text{ km}^2$ , which favourably compares with the observational estimates given by *Lemke et al.* [2007] of  $7 \cdot 10^6 \text{ km}^2$  and  $15 \cdot 10^6 \text{ km}^2$ , respectively. Antarctic sea ice extent in KCM exhibits a larger range of  $3\text{--}20 \cdot 10^6 \text{ km}^2$  and is similar to the *Lemke et al.* [2007] estimate of  $3\text{--}19 \cdot 10^6 \text{ km}^2$ .

### 3. Multidecadal and Multicentennial Variability

[6] Surprisingly, the level of decadal to centennial variability in Northern Hemisphere surface air temperature (SAT) simulated by KCM is consistent with that obtained from the *Mann and Jones* [2003] reconstruction (not shown). This point will be discussed in a forthcoming paper. Here we focus in the following on the MOC variability. We computed first an index of the MOC strength as the maximum of the overturning streamfunction at  $30^{\circ}\text{N}$ . The annual index (Figure 1b) has a mean value of  $13.6\text{Sv}$  and exhibits rich variability on different timescales. MOC strength varies between about  $11\text{--}18\text{Sv}$ , and decadal to centennial variability is obvious with strong year-to-year fluctuations superimposed. The corresponding spectrum (Figure 1c) is red up to centennial timescales, which is expected given the involvement of intermediate and deep ocean dynamics in MOC variability. At decadal timescales, a broad and statistically significant (above the 99% level) peak (relative to the spectrum of a fitted AR1-process) is seen at periods of about  $50\text{--}100$  years. Apparently, multidecadal MOC variability simulated by KCM seems to constitute a true oscillatory mode of the coupled ocean-atmosphere system. A second region of enhanced variability is found at centennial timescales, with maximum power at periods of about  $300\text{--}400$  years. Whether or not the latter is a true oscillatory mode of the coupled system remains unclear, because the length of the integration does not allow the investigation of enough realisations. The two regions of enhanced power, however, are clearly separated from each other.

[7] Since we are interested only in long-term MOC variability, we averaged the annual data to 5-year means in the subsequent analyses. In order to separate the two types of variability we employ temporal filtering: first, a low-pass filter retaining variability with periods longer than 90 years is applied to investigate multicentennial variability (Figure 2a), and second, a band-pass filter retaining variability with periods between 30 and 90 years to study multidecadal variability (Figure 2b). Different statistical methods such as Singular Spectrum Analysis (SSA) were applied to separate the two types of variability, but the results did not change in any significant way. The corresponding standard deviations are: 1) annual MOC index =  $1.02\text{Sv}$ , 2) band-pass filtered (multidecadal) index =  $0.46\text{Sv}$ , and 3) low-

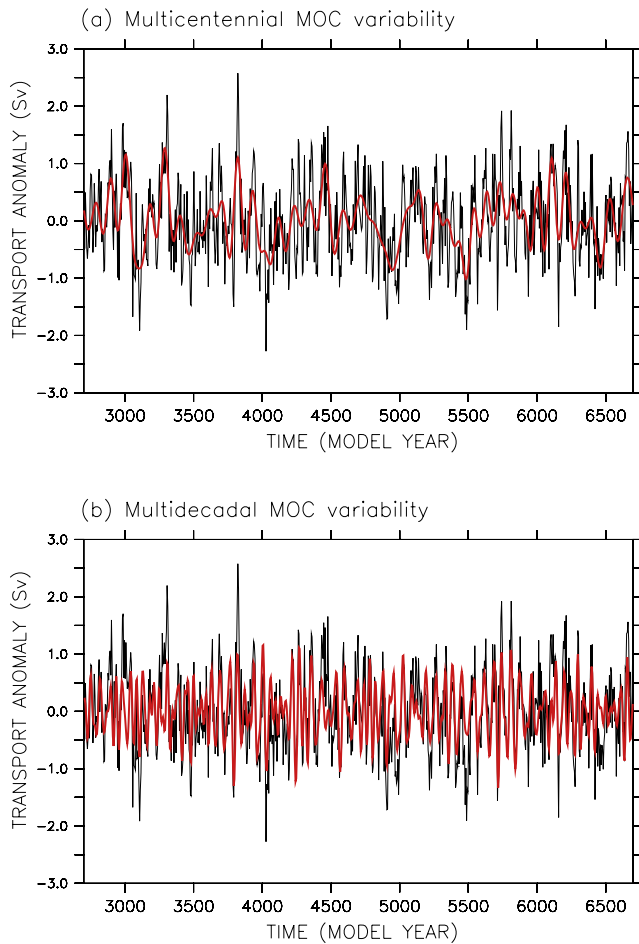


**Figure 2.** (a) MOC strength anomalies [Sv] based on 5-year averages and the low-pass filtered version that highlights the multicentennial variability, (b) same as in Figure 2a but showing instead of the low-pass filtered the band-pass filtered version that highlights the multidecadal variability.

pass filtered (multicentennial) index =  $0.43\text{Sv}$ . Composites for the overturning streamfunction were computed using the filtered timeseries, applying a one standard deviation threshold. The high minus low composite for the multicentennial variability (Figure 3a) yields an intensified North Atlantic Deep Water (NADW) cell that extends to deeper levels. The strongest change is simulated at  $30^\circ\text{S}$ , suggesting multicentennial MOC variability is driven in the Southern Hemisphere. The composite for the multidecadal variability shows a similar strengthening of the NADW cell (Figure 3b). The maximum change, however, is simulated near  $40^\circ\text{N}$  suggesting a northern control of multidecadal variability, as in many other models.

[8] The SAT pattern associated with the multicentennial and multidecadal variability was computed using 5-year means by linear regression upon the corresponding filtered MOC timeseries. The SAT regression patterns (Figures 4a and 4b) support the picture that multicentennial variability is driven in the Southern Hemisphere, while multidecadal variability originates in the Northern Hemisphere. The multicentennial SAT pattern (Figure 4a) has strongest load-

ings in the South Atlantic, with maximum changes of more than  $2^\circ\text{C}/\text{Sv}$ . Explained variances relative to the 5-year means are typically in the range of 10–20% in this region. The North Atlantic is mostly covered by weaker positive anomalies extending to about  $60^\circ\text{N}$  (please note the non-linear scale). This pattern, although clearly dominated by the SAT anomalies in the South Atlantic, projects onto the inter-hemispheric Atlantic SST dipole described above. Explained variances in the North Atlantic, however, are generally low, with the exception of the region  $40\text{--}50^\circ\text{N}$ . The SAT pattern associated with the multidecadal variability does also project on the inter-hemispheric SST dipole but is clearly dominated by SAT anomalies in the North Atlantic (Figure 4b). In comparison with the multicentennial pattern, the North Atlantic anomalies are much stronger relative to those in the South Atlantic and they extend farther north into the Arctic. Explained variances are rather small and generally well below 10%, except in a region extending from the Iberian Peninsula into the Tropics. The Atlantic SST-dipole index as defined by *Latif et al.* [2006] seems to monitor both types of MOC variability, although SAT generally exhibits a relatively bad signal-to-noise ratio.

[9] We next investigate the impact of MOC variability on sea ice, again by computing linear regressions (Figures 4c and 4d). The multicentennial MOC variability is connected to strong changes in Southern Hemisphere sea ice fraction (Figure 4c). In the Weddell Sea, changes can amount to about  $25\%/Sv$ . The multidecadal variability in Southern Hemisphere sea ice extent is event-like (not shown), but clearly related to the multidecadal MOC variability, with explained variances of more than 20% in parts of the

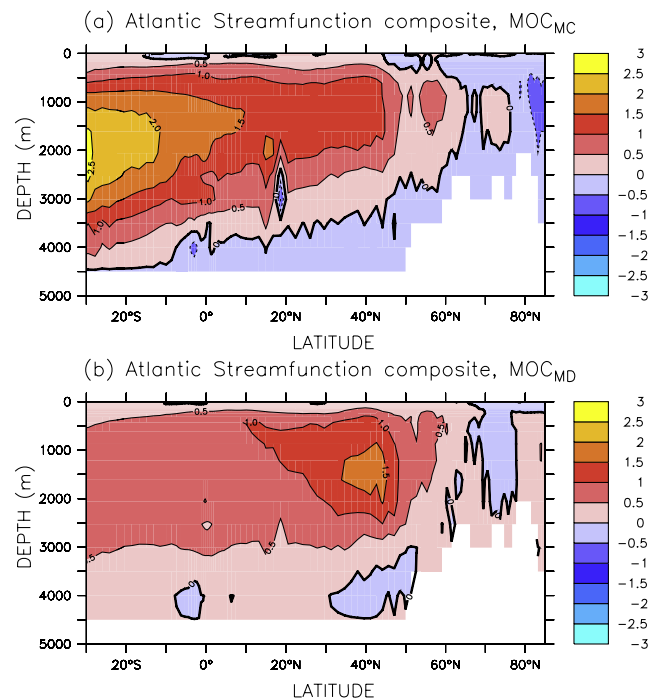


**Figure 3.** MOC (high minus low) composite [Sv] for strong phases of (a) multicentennial and (b) multidecadal MOC variability. Composites were computed applying a one-standard deviation criterion using the reconstructed time series shown in Figure 2.

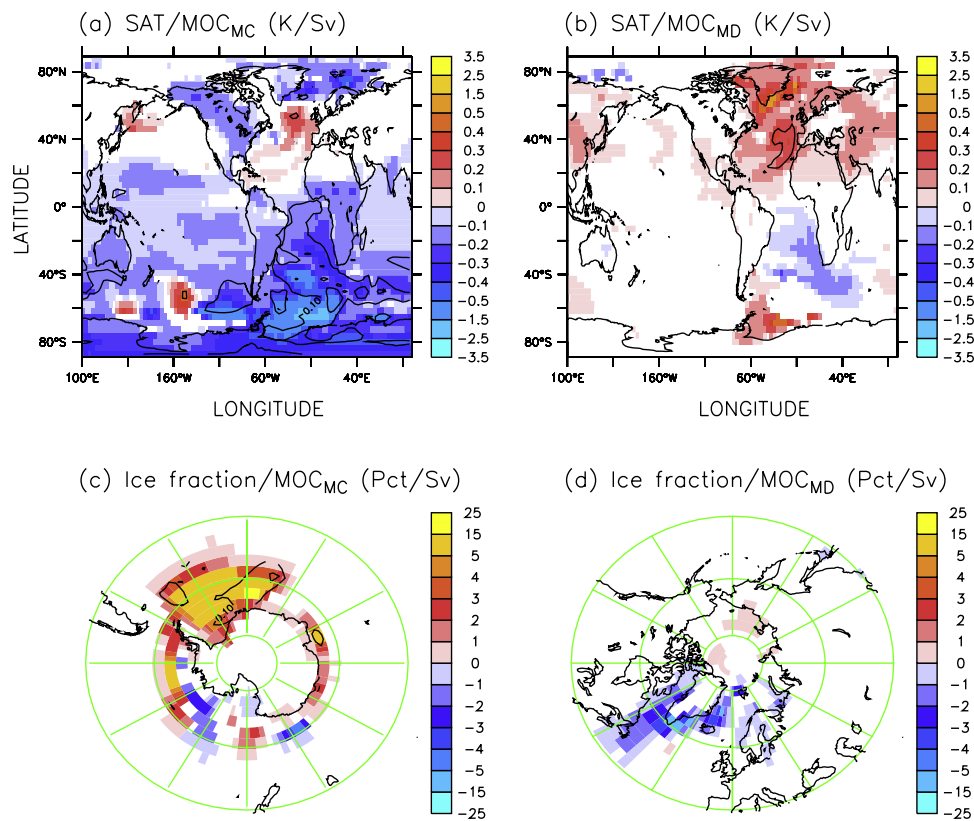


**Figure 4.** Maps of linear regression coefficients for SAT [K/Sv] and sea ice [%/Sv] upon (a) and (c) the low-pass filtered MOC strength highlighting the multicentennial variability and (b) and (d) the band-pass filtered MOC strength highlighting the multidecadal variability. Shading denotes the regression values; contours denote explained variances (contour interval amounts to 0.1).

Weddell Sea. During phases of strong multicentennial events maximum sea ice extent changes from about  $15$  to almost  $20 \cdot 10^6$  km<sup>2</sup>, a change of 25%. Such a strong internal fluctuation is much larger than the observed increase in Antarctic sea ice extent since the late 1970s of about  $0.1$ – $0.2 \cdot 10^6$  km<sup>2</sup>. The Northern Hemisphere sea ice does not display any strong centennial-timescale variability (not shown). In contrast, sea ice regressions (Figure 4d) associated with multidecadal MOC variability yield coherent changes in the Northern Hemisphere of the order of several percent/Sv, but are not coherent in the Southern Hemisphere (not shown). In summary, a clear timescale separation exists in the spatial structures associated with multidecadal and multicentennial MOC variability.

#### 4. Discussion

[10] Pronounced multidecadal and multicentennial variability in the Atlantic meridional overturning circulation (MOC) is simulated in a multimillennial control integration of the Kiel Climate Model (KCM). Multicentennial MOC variability is controlled by Southern Hemisphere and multidecadal variability by Northern Hemisphere processes. The centennial-scale variability shares many common aspects with that found in previous ocean model studies [e.g., Mikolajewicz and Maier-Reimer, 1990; Pierce et al., 1995; Drijfhout et al., 1996; Osborn, 1997], while the decadal-scale variability is consistent with that simulated

in other coupled models [e.g., Delworth and Mann, 2000; Knight et al., 2005, 2006]. Details on the mechanisms, specifically the coupled ocean-atmosphere-sea ice interactions will be given in a forthcoming paper.

[11] The results are important concerning anthropogenic climate change. Schmittner et al. [2005] estimated from climate model projections that the anthropogenic MOC weakening by the end of the 21st century will be of the order of 25% or about 4Sv. The anthropogenic signal, however, will be superimposed by internal low-frequency variability. Trend distributions from KCM indicate that the projected anthropogenic weakening is well within the range of internal variability over the next 50 years, when assuming a linear decline. A trend of  $\pm 4$ Sv/century, however, is not simulated. If the model results are realistic, other expected anthropogenic signals will be also masked by internal variability, especially in the Southern Hemisphere. The projected change of Southern Hemisphere sea ice extent in response to global warming [Meehl et al., 2007], for instance, is of the same order of magnitude as the level of internal multicentennial variability in KCM. The forcing by stratospheric ozone changes or intrinsic decadal variability in the Southern Annular Mode (SAM), however, has also to be considered in this context. It is likely to be very hard to get good evidence of the existence of variability such as the multicentennial mode in instrumental or paleo-data. As such, we do not know how realistic the model's representation of this type of variability is. Nevertheless, the results

show the potential for internally generated variability to be significant on these timescales, which are those of climate change. Finally, it is important to note the recent strong decline in Arctic sea ice may contain a strong contribution from internal variability, since the latter may also exacerbate anthropogenic climate change signals.

[12] **Acknowledgments.** The EU projects ENSEMBLES and DYNAMITE and the German project NORDATLANTIK of the German Federal Ministry of Research (BMBF) supported this work. The model integrations were performed at the DKRZ Hamburg and the Computer Centre at Kiel University. This paper is a contribution to the Excellent Cluster “The Future Ocean”.

## References

- Cunningham, S. A., et al. (2007), Temporal variability of the Atlantic meridional overturning circulation at 26.5°N, *Science*, 317, 935–938.
- Delworth, T. L., and M. E. Mann (2000), Observed and simulated multidecadal variability in the Northern Hemisphere, *Clim. Dyn.*, 16, 661–676.
- Delworth, T., S. Manabe, and R. J. Stouffer (1993), Interdecadal variations of the thermohaline circulation in a coupled ocean-atmosphere model, *J. Clim.*, 6, 1993–2011.
- Drijfhout, S., C. Heinze, M. Latif, and E. Maier-Reimer (1996), Mean circulation and internal variability in an ocean primitive equation model, *J. Phys. Oceanogr.*, 26, 559–580.
- EPICA Community Members, (2006), One-to-one coupling of glacial climate variability in Greenland and Antarctica, *Nature*, 444, 195–198.
- Folland, C. K., T. N. Palmer, and D. E. Parker (1986), Sahel rainfall and worldwide sea temperatures, 1901–85, *Nature*, 320, 602–607, doi:10.1038/320602a0.
- Kanzow, T., et al. (2007), Observed flow compensation associated with the MOC at 26.5°N in the Atlantic, *Science*, 317, 938–941, doi:10.1126/science.1141293.
- Knight, J. R., R. J. Allan, C. K. Folland, M. Vellinga, and M. E. Mann (2005), A signature of persistent natural thermohaline circulation cycles in observed climate, *Geophys. Res. Lett.*, 32, L20708, doi:10.1029/2005GL024233.
- Knight, J. R., C. K. Folland, and A. A. Scaife (2006), Climate impacts of the Atlantic Multidecadal Oscillation, *Geophys. Res. Lett.*, 33, L17706, doi:10.1029/2006GL026242.
- Latif, M., et al. (2004), Reconstructing, monitoring, and predicting multidecadal-scale changes in the North Atlantic thermohaline circulation with sea surface temperature, *J. Clim.*, 17, 1605–1614.
- Latif, M., et al. (2006), Is the thermohaline circulation changing?, *J. Clim.*, 19, 4631–4637.
- Latif, M., et al. (2007), Decadal to multidecadal variability of the Atlantic MOC: Mechanisms and predictability, in *Ocean Circulation: Mechanisms and Impacts: Past and Future Changes of Meridional Overturning*, *Geophys. Monogr. Ser.*, vol. 173, edited by A. Schmittner, J. C. H. Chiang, and S. R. Hemming, pp. 149–166, AGU, Washington, D. C.
- Lenke, P., et al. (2007), Observations: Changes in snow, ice and frozen ground, in *Climate Change 2007: The Physical Science Basis. Contribution of Working Group I to the Fourth Assessment Report of the Intergovernmental Panel on Climate Change*, edited by S. Solomon et al., chap. 4, pp. 339–383, Cambridge Univ. Press, Cambridge, U. K.
- Madec, G. (2008), NEMO reference manual, ocean dynamics component: NEMO-OPA. Preliminary version, *Note Pole Model. 27*, Inst. Pierre-Simon Laplace, Paris.
- Madec, G., P. Delecluse, M. Imbard, and C. Lévy (1998), OPA 8.1 Ocean General Circulation Model reference manual, *Note Pole Model. 11*, 91 pp., Inst. Pierre-Simon Laplace, Paris.
- Mann, M. E., and P. D. Jones (2003), Global surface temperatures over the past two millennia, *Geophys. Res. Lett.*, 30(15), 1820, doi:10.1029/2003GL017814.
- Meehl, G. A., et al. (2007), Global climate projections, in *Climate Change 2007: The Physical Science Basis. Contribution of Working Group I to the Fourth Assessment Report of the Intergovernmental Panel on Climate Change*, edited by S. Solomon, chap. 10, pp. 749–845, Cambridge Univ. Press, Cambridge, U. K.
- Mikolajewicz, U., and E. Maier-Reimer (1990), Internal secular variability in an ocean general circulation model, *Clim. Dyn.*, 4, 145–156.
- Osborn, T. J. (1997), Thermohaline oscillation in the LSG OGCM: Propagating anomalies and sensitivity to parameterizations, *J. Phys. Oceanogr.*, 27, 2233–2255.
- Park, W., et al. (2008), Tropical Pacific climate and its response to global warming in the Kiel Climate Model, *J. Clim.*, in press.
- Pierce, D. W., T. P. Barnett, and U. Mikolajewicz (1995), Competing roles of heat and freshwater flux in forcing thermohaline oscillations, *J. Phys. Oceanogr.*, 25, 2046–2064.
- Roeckner, E., et al. (2003), The atmospheric general circulation model ECHAM5. Part I: Model description, *Rep. 349*, 127 pp., Max Planck Inst. for Meteorol., Hamburg, Germany.
- Schmittner, A., M. Latif, and B. Schneider (2005), Model projections of the North Atlantic thermohaline circulation for the 21st century assessed by observations, *Geophys. Res. Lett.*, 32, L23710, doi:10.1029/2005GL024368.
- Schmittner, A., J. C. H. Chiang, and S. R. Hemming (Eds.) (2007), *Ocean Circulation: Mechanisms and Impacts*, *Geophys. Monogr. Ser.*, vol. 173, 392 pp, AGU, Washington, D. C.
- Stocker, T. F. (1998), The seesaw effect, *Science*, 282, 61–62.
- Timmermann, A., M. Latif, R. Voss, and A. Grötzner (1998), Northern Hemispheric interdecadal variability: A coupled air-sea mode, *J. Clim.*, 11, 1906–1931.
- Valcke, S. (2006), OASIS3 user guide, *PRISM Tech. Rep. 3*, 64 pp., Partnership for Res. Infrastructures in Earth Syst. Model., Toulouse, France. (Available at [http://www.prism.enes.org/Publications/Reports/oasis3\\_UserGuide\\_T3.pdf](http://www.prism.enes.org/Publications/Reports/oasis3_UserGuide_T3.pdf)).
- Zhang, R., and T. L. Delworth (2006), Impact of Atlantic multidecadal oscillations on India/Sahel rainfall and Atlantic hurricanes, *Geophys. Res. Lett.*, 33, L17712, doi:10.1029/2006GL026267.

M. Latif and W. Park, Leibniz-Institut für Meereswissenschaften, Düsternbrooker Weg 20, Kiel, Germany. (mlatif@ifm-geomar.de)